FINAL TECHNICAL REPORT

NASA GRANT NO. NAG8-738

"Studies of the Evolution of the X-Ray Emission of Clusters of Galaxies"

July 1, 1988 to December 31, 1989

Submitted by

J. Patrick Henry
University of Hawaii
Institute for Astronomy
2680 Woodlawn Drive
Honolulu, Hawaii 96822

FINAL TECHNICAL REPORT FOR GRANT NAG8-738

by

J. Patrick Henry, Principal Investigator

The X-ray luminosity function of clusters of galaxies was determined at different cosmic epoches using data from the *Einstein Observatory* Extended Medium Survey. The sample consisted of 67 X-ray selected clusters that were grouped into three redshift shells. Evolution was detected in the X-ray properties of clusters. The present volume density of high luminosity clusters was found to be greater than it was in the past. This result is the first convincing evidence for evolution in the X-ray properties of clusters.

The enclosed paper reporting this work has been accepted in the Astrophysical Journal (Letters). Investigations into the constraints provided by these data on various Cold Dark Matter models are underway.

THE EMSS DISTANT CLUSTER SAMPLE: X-RAY COSMOLOGICAL EVOLUTION[1]

I. M. Gioia[2,3], J. P. Henry[4], T. Maccacaro[2,5], S. L. Morris[6], J. T. Stocke[7], and A. Wolter[2]

2) Harvard-Smithsonian Center for Astrophysics, Cambridge, MA

3) Istituto di Radioastronomia del CNR, Bologna, Italy

4) Institute for Astronomy, University of Hawaii, Honolulu, HI

5) Osservatorio Astronomico di Bologna, Italy

6) The Obs. of the Carnegie Institute of Washington, Pasadena, CA

7) Center for Astrophysics and Space Astronomy, Boulder, CO

[1]This paper uses data obtained at the Multiple Mirror Telescope Observatory (MMTO), which is operated jointly by the University of Arizona and the Smithsonian Institution, and at the University of Hawaii 2.2m Telescope.

Abstract

The X-ray luminosity function of clusters of galaxies is determined at different cosmic epochs using data from the *Einstein Observatory* Extended Medium Sensitivity Survey. The sample consists of 67 X-ray selected clusters that have been grouped in three redshift shells. Evolution is detected in the X-ray properties of clusters. The present volume density of high luminosity clusters is found to be *greater* than it was in the past. Given the still limited data set this result should be regarded as preliminary. It can be interpreted as the consequence of either *luminosity* evolution or modest *density* evolution.

Keywords: Clusters of Galaxies: Luminosity Function - Evolution - X-rays

I. Introduction

The study of distant clusters of galaxies provides important information on their formation and evolution. Investigations of the X-ray evolution have almost always proceeded by making observations of clusters of galaxies selected in the optical (Henry et al. 1982; Henry and Lavery, 1984). There is currently little evidence for evolution in X-ray luminosity or temperature for distant optically selected clusters. Surprisingly, for the only two distant systems studied in detail, the cluster 0016+16 at z = 0.541 (White, Silk and Henry, 1981) and the cluster around 3C295 at z = 0.461 (Henry and Henriksen, 1986), the X-ray properties were found to be similar to those of nearer rich clusters. However, these apparent similarities between distant and nearby systems might be primarily due to a selection effect. Since distant clusters selected optically are chosen because they are especially rich, these clusters may be among the few which have already undergone a considerable amount of dynamical evolution. It is almost impossible to avoid or quantify biases in optically selected samples because they are chosen by eye. Even investigators who presently make catalogs by scanning plates and who select the galaxies and clusters by using rigorous algorithms are faced with the problem of contamination by foreground galaxies and stars.

X-ray selection does not have these biases, even though different selection effects are present. There may be a preference for the detection of high surface brightness systems as well as clusters with deep potential wells. Since the vast majority of the clusters known today have been selected in the optical, it is vital to investigate the properties of a cluster sample extracted from an X-ray survey for a different approach to the understanding of cluster

formation and evolution. A Hubble constant $H_0 = 50$ km s^{-1} Mpc^{-1}, and a Friedmann universe with a deceleration parameter $q_0 = 0$ is assumed throughout this *Letter*.

II. The Sample

The sample of clusters of galaxies used in this study is extracted from the *Einstein* Extended Medium Sensitivity Survey (EMSS). A detailed description of the survey sources, the selection criteria, the detection algorithm, the computation of the X-ray flux and other parameters is given in Gioia et al. 1990. We recall here that the EMSS is a flux limited sample consisting of 835 sources serendipitously detected in Imaging Proportional Counter (IPC) fields at high Galactic latitude, with limiting sensitivities ranging from 5×10^{-14} to 3×10^{-12} erg cm^{-2} s^{-1} in the 0.3–3.5 keV energy band. A detailed discussion of the identifications, as well as presentation of finding charts, spectral and photometric data is in preparation and will be presented elsewhere (Stocke et al. 1990, in preparation; Maccacaro et al. 1990, in preparation). For the purpose of this study we have considered only sources with declination greater than $-40°$ (accessible from Mauna Kea) and flux greater than 1.5×10^{-13} erg cm^{-2} s^{-1} in a $2.'4 \times 2.'4$ detection cell (to reduce the number of still unidentified sources). Adopting these criteria the survey contains 733 sources and is 97% identified. There are 93 sources identified with clusters of galaxies. Since most nearby clusters were observed as a target of IPC observations they were not available to be detected serendipitously by the EMSS, so this sample is not complete at the low end of the redshift distribution. For this study we have chosen to use only those clusters in our sample with a redshift greater than 0.14. This value roughly corresponds to Abell Distance classes 5-6. Since the majority of

the Abell clusters chosen as the target of the IPC observations belong to Distance Class 3 or less, we feel comfortable in using the value of 0.14 as a lower limit in redshift. The resulting sample contains 67 objects. It is the most numerous sample of distant clusters of galaxies extracted from a flux limited survey of "faint" X-ray sources: i.e. the sample is defined exclusively by its X-ray properties. The precise knowledge of the area of sky searched for X-ray sources and of the limiting sensitivity pertaining to each area allows us to derive the cluster X-ray luminosity function. In the redshift range $0.14 \leq z < 0.20$ there are 20 clusters of which only 4 are in the Abell catalog. The X-ray luminosities of objects in this shell are all greater than 10^{44} erg s^{-1}. Since clusters with this luminosity are almost exclusively Abell clusters at lower redshift, it is somewhat surprising that we find so few of them. Although our clusters are mostly not Abell clusters, it is premature to discuss the implications of these results on the completness of the Abell catalog until more optical work is completed on our clusters.

Even though the EMSS is statistically well defined, there are still a number of effects in the data which must be taken into account. These effects are absorption by the Milky Way, the different redshifts of the sources, the different sky coverage for different flux limits, and the correction for lost flux due to the finite source size (the EMSS uses a detection cell of 2.′4 × 2.′4). We discuss the corrections we have applied to take into account each of these effects on our data. We note here that the EMSS uses the so called M-DETECT algorithm to find sources. In this method the background is computed from a global map of the detector so that sources are not lost because their extended flux distribution mistakenly increases the

apparent background around them (see Gioia et al. 1990 for a detailed discussion).

The flux from each source has been corrected for absorption using the neutral Hydrogen values from the survey of Stark et al. (1984). Most of the sky was observed through a small range of N_H which results in a negligible bias (see Zamorani et al. 1988, and Maccacaro et al. 1988). K-corrections are small for our sample. Assuming a Raymond-Smith spectrum at a redshift of 0.5, the correction is always within 15% of unity for temperatures between 2 and 10 keV (Burg, 1989 private communication) and is less at smaller redshifts. Therefore, for simplicity we used K-corrections calculated assuming a power law spectrum with energy index of 0.5, which roughly approximates a 6 keV thermal spectrum in our 0.3−3.5 keV energy band. The sky coverage North of $-40°$ declination has been calculated adopting the same spectrum and procedures used to determine the flux of the clusters, i.e. using only the counts in the detection cell without applying any correction for the point response function or the mirror scattering.

The largest correction is for the effect of the finite size of the X-ray emission in clusters. This correction will be used in two places: first to calculate the true luminosity of a cluster when only its detection cell flux and redshift are known, and second to determine the amount of flux that would appear in the detection cell at different redshifts during the calculation of the maximum observable redshift (see Section III) in the derivation of the luminosity function. We adopt the β model for the cluster surface brightness, that is

$$I(\theta) = \frac{I_0}{[1 + (\theta/\theta_0)^2]^{(3\beta - 1/2)}}$$

From Jones and Forman (1984) we adopt $\beta = 2/3$. Then integrating over the square detection

cell between 0 and θ_D we obtain the observed flux:

$$F_{obs} = 4 \int_0^{\theta_D} d\theta_x \int_0^{\theta_D} d\theta_y \; I(\theta)$$

where θ_D is the angular half-size of the detection cell (1.′2) we obtain:

$$F_{obs} = 2\pi I_0 \theta_0^2 f(\frac{\theta_D}{\theta_0})$$

where

$$f(\frac{\theta_D}{\theta_0}) = \frac{1}{2} + \frac{1}{\pi} \sin^{-1}[\frac{(\theta_D^2/\theta_0^2 - 1)^2 - 2}{(\theta_D^2/\theta_0^2 + 1)^2}] \tag{1}$$

is the fraction of the total flux in the detection cell. We determine θ_0 using the 18 Piccinotti et al. (1982) clusters (HEAO1-A2 experiment) which have IPC imaging data and which are not so large that they extend beyond the IPC ribs. This sample is X-ray selected and seems to be the most comparable with our sample. For these 18 clusters, we calculate the average fraction of the total flux (as determined by Piccinotti et al.) which is detected by the EMSS detection cell if each cluster were at a fiducial redshift. The arbitrary fiducial redshift was chosen to be 0.35 which gives $D_A \times \theta_D = 0.5$ Mpc, where D_A is the angular diameter distance. At this redshift, the average fraction of flux of the Piccinotti et al. objects that would be in the detection cell is equal to 0.43 with a large dispersion ($\sigma = 0.2$). No obvious dependence is found between this fraction and the X-ray luminosity of the clusters. From (1), $D_A \times \theta_0 = 0.37$ Mpc. Equation (1) with this value of θ_0 is used to correct the observed luminosity to the total luminosity. The redshift dependence of I_0 and θ_0 are:

$$I_0(z) = \frac{I_0(1 + z_{obs})^4}{(1 + z)^4}$$

$$\theta_0(z) = \frac{\theta_0 D_A(z_{obs})}{D_A(z)}$$

where z_{obs} is the redshift of the cluster. We assume that θ_0 and β do not evolve with redshift. Performing a similar integral over the detection cell for the cluster at an arbitrary redshift gives

$$F(z) = F_{obs} \frac{D_L^2(z_{obs})}{D_L^2(z)} \frac{f(D_A(z)\theta_D/D_A\theta_0)}{f(D_A(z_{obs})\theta_D/D_A\theta_0)} \tag{2}$$

where D_L is the luminosity distance. This expression is used in the calculation of the maximum redshift at which a given object could have been detected. It reduces to the point source result in the limit that the size of the detection cell is much larger than that of the cluster.

III. The X-ray Luminosity Function

In this section we derive and discuss the X-ray Luminosity Function (XLF) for clusters of galaxies computed in three different redshift shells defined by z_{low} and z_{high}. A non-parametric representation of the XLF is first obtained using the $1/V_a$ method of Avni and Bahcall (1980) a generalization of the $1/V_{max}$ method (Schmidt 1968) when several complete samples are analyzed. For each cluster falling in one of the three $z_{low}-z_{high}$ shells defined later we computed the maximum redshift (z_{max}) at which the source could have been seen taking into account the solid angle observed at different limiting sensitivities. The maximum volume in which the cluster could have been detected depends on the redshift of the shell under consideration, the luminosity of the cluster and the sky coverage of the EMSS. The search volume for a given cluster, V_a, is the sum of all volumes lying between the minimum redshift z_{low} of the shell under consideration and the lesser of the maximum shell redshift z_{high} or the maximum redshift z_{max} at which the source could have been seen for each different

sensitivity limit. The individual contributions have been binned by log luminosity to create the differential XLF N(L) integrated in independent bins 0.3 wide in ΔlogL. For each bin we have:

$$N(L) = \sum_{j=1}^{n} \frac{1}{V_{a,j}\Delta L}$$

where n is the number of objects in that bin. The results are shown in Fig. 1, where the three panels give the XLF's in redshift shells as indicated. There are 20 clusters with redshift $0.14 \leq z < 0.20$, 26 clusters with redshift $0.20 \leq z < 0.30$ and 21 clusters with redshift $0.30 \leq z < 0.60$. The 1σ error bars associated with each bin are determined from the number of objects contributing to that bin and have been computed using Poisson statistics (Regener, 1951).

We then consider a parametric representation of the luminosity function of the form

$$\frac{dN}{dL_{44}} = KL_{44}^{-\alpha} Mpc^{-3} L_{44}^{-1}$$

where L_{44} is the X-ray luminosity in units of 10^{44} erg s^{-1} and K is the normalization coefficient expressed in units of Mpc^{-3} L_{44}^{-1} . The maximum likelihood method (see Murdoch, Crawford and Jauncey, 1973, and references therein) has been applied to the unbinned data to estimate the best fit slopes which are given in Table 1 with there associated 1σ errors. The fits have been computed in each redshift range between the minimum observable luminosity L_{min} and infinite luminosity.

Table 1

Parametric Representation of the Cluster X-ray Luminosity Function

z	α	$K(Mpc^{-3}L_{44}^{-1})$	$logL_{min}$
$0.14-0.20$	2.09 ± 0.20	$(7.19 \pm 0.58) \times 10^{-7}$	42.90
$0.20-0.30$	2.63 ± 0.22	$(10.8 \pm 1.56) \times 10^{-7}$	43.30
$0.30-0.60$	3.09 ± 0.27	$(12.2 \pm 4.46) \times 10^{-7}$	43.80

The normalization coefficient K has been computed by requiring that the number of expected objects equals the number of observed objects. Errors on K have been determined by letting α assume the 1σ extremes in each case. A steepening of the slope is observed at higher redshifts. This change is best seen in Fig. 2 where the differential XLF's for clusters in the lowest shell ($0.14 \leq z < 0.20$) and in the highest shell ($0.30 \leq z < 0.60$) are plotted. The difference between the two slopes is significant at the 3 σ confidence level.

We note that no cluster with log $L_x > 45.2$ has been detected at low redshift ($0.14 \leq z < 0.20$). Clearly these clusters, which have been detected at higher redshift, could have been detected at lower redshift. However the available volume in the low redshift shell is much smaller than the volume in the higher redshift shells. Only one cluster is expected in the bin centered at log $L_x = 45.35$. Thus the absence of log $L_x > 45.2$ clusters in the low$-$z shell is not significant and is not necessarily indicative of a break in the XLF of low redshift clusters. It is of interest to compare our lowest redshift XLF with that of Piccinotti et al. (1982) even though their sample was at a lower redshift and in a different energy band. The two slopes agree (2.09 vs. 2.15) within the errors. With the same 6 keV thermal spectrum we used

previously to compute our fluxes, we find that the Piccinotti normalization, converted from their 2-10 keV band to our 0.3-3.5 keV, is 2.1 $\pm$ 1.6 times smaller than ours. That is we essentially agree within the errors.

IV. Discussion

Even if our result is significant only at the 3σ level we believe we have the first convincing evidence for evolution in the X-ray properties of clusters. Note that the slopes are independent of the correction applied for the flux lost outside of the detection cell because all the sources in each shell are at approximately the same redshift. The XLF which characterizes high redshift clusters ($0.30 \leq z < 0.60$) is significantly steeper than the XLF of low redshift clusters ($0.14 \leq z < 0.20$). This trend is supported by the intermediate XLF ($0.20 \leq z < 0.30$). We have assumed that θ_0 does not evolve. If, however, the core radius decreases with redshift, as would be expected in an hierarchical scenario, then we would make a smaller correction for the flux lost outside the detection cell, would have fewer high luminosity clusters, and would find even stronger evolution than we do.

The luminosity range covered by our data is rather limited and prevents a detailed analysis of the shape and kind of cosmological evolution. Furthermore, there are still 19 sources unidentified which could modify the results presented in this *Letter*. However evolution seems present only at high luminosities ($\log L_x \geq 44.7$). At lower luminosities ($44.2 \leq log L_x < 44.7$) no significant difference exists as a function of redshift. This behavior is suggestive of a *luminosity dependent* evolution such that the volume density of high luminosity clusters (log

$L_x \geq 44.7$) is higher at the present epoch than at epochs corresponding to redshifts of about 0.5. The volume density of low luminosity clusters has remained unchanged. Presumably our power law characterization of the data could be naive and a luminosity function with a break analogous to a Schechter function could be more appropriate. In this case, the different slopes observed could be the result of either *luminosity evolution*, with the break shifted to a higher luminosity for the lower redshift clusters, or a modest *density evolution*. In the latter case the apparent change in slope would result because the high redshift sample, with intrinsically more luminous clusters in the mean, has more objects drawn from above the break relative to the low redshift samples.

The basic conclusion is that there is good evidence for a *difference between the X-ray luminosity function at high and low redshift.* This difference goes in the *opposite sense* to that anticipated by Kaiser (1986) who predicted density evolution in the sense that there would have been a higher volume density of X-ray clusters in the past. By contrast, the evidence for evolution we have found, that is fewer clusters in the past, is in the *same sense* as anticipated by Perrenod (1980) (see also Cavaliere and Colafrancesco, 1988).

After this paper had been submitted we received a preprint from Edge et al. (1990) who found a similar result from an independent data set.

We would like to thank R. Giacconi and R. Burg for many interesting discussions when this work was at an early stage of preparation, and G. Zamorani for many helpful suggestions and comments. This work has received partial financial support from NASA contract NAS8-

30751, NASA Grants NAG8-738 and NAG5-1256, NSF Grant AST-8715983, and from the Smithsonian Institution Scholarly Studies Grants SS48-8-84 and SS88-3-87.

References

Avni, Y., and Bahcall, J.N., Ap. J., 235, 694.

Cavaliere, A., and Colafrancesco, S., 1988, Ap. J., 331, 660.

Edge, A.C., Stewart, G.C., Fabian, A.C., and Arnaud, K.A., 1990, submitted to M.N.R.A.S.

Gioia, I.M., Maccacaro, T., Schild, R.E., Wolter, A., Stocke, J.S., Morris, S.L., and Henry, J.P., 1990, Ap. J. Suppl., 72, in press.

Henry, J.P., Soltan, A., Briel, U., and Gunn, J.E., 1982, Ap. J., 262, 1.

Henry, J.P., and Henriksen, M.J., 1986, Ap. J., 301, 689.

Henry, J.P., and Lavery, R.J., 1984, Ap. J., 280, 1.

Jones, C.J., and Forman, W.R., 1984, Ap. J., 276, 38.

Kaiser, N., (1986), Mon. Not. Roy. Astr. Soc., 222, 323.

Maccacaro, T., Gioia, I.M., Wolter, A., Zamorani, G., and Stocke, J.T., 1988, Ap. J., 326, 680.

Murdoch, H.S., Crawford, D.E., and Jauncey, D.L., 1973, Ap. J., 183, 1.

Perrenod, S.C., 1980, Ap. J., 236, 373.

Pesce, J.E., Fabian, A.C., Edge, A.C., and Johnstone, R.M., 1990, Mon. Not. Roy. Astr. Soc., in press.

Piccinotti, G., Mushotzky, R.F., Boldt, E.A.,Holt, S.S., Marshall, F.E., Serlemitsos, P.J., and Shafer, R.A., 1982, Ap. J., 253, 485.

Regener, V.H., 1951, Phys. Rev, 84, 161L.

Schmidt, M., 1968, Ap. J., 151, 393.

Stark, A.A., Heiles, C., Bally, J., and Limke, R., 1984, Bell Labs, privately distributed magnetic tape.

White, S.D.M., Silk, J., and Henry, J.P., 1981, Ap. J. (Letters) 251, L65.

Zamorani, G., Gioia, I.M., Maccacaro, T., and Wolter, A., 1988, Astron. and Astrophys., 196, 39.

Figure Captions

Fig. 1 - The differential luminosity functions of clusters in the three redshift shells: a) $0.14 \leq z < 0.20$; b) $0.20 \leq z < 0.30$ and c) $0.30 \leq z < 0.60$.

Fig. 2 - A comparison of the differential luminosity functions for the lowest (open squares) and the highest (filled dots) redshift shells. The straight lines represent maximum likelihood fits to the individual unbinned data. The dot-dashed line is the fit for the lowest redshift shell and the solid line is the fit for the highest redshift shell.

Author Addresses

I.M. Gioia, T.Maccacaro, and A. Wolter
Harvard Smithsonian Center for Astrophysics
60 Garden Street, Cambridge, MA 02138

J.P. Henry
Institute for Astronomy
University of Hawaii
2680 Woodlawn Drive, Honolulu, HI 96822

S.L. Morris
The Observatories of the Carnegie Institute of Washington
813 Santa Barbara Street, Pasadena, CA 91101

J.T. Stocke
Center for Astrophysics and Space Astronomy
University of Colorado
Campus Box 391, Boulder, CO 80309

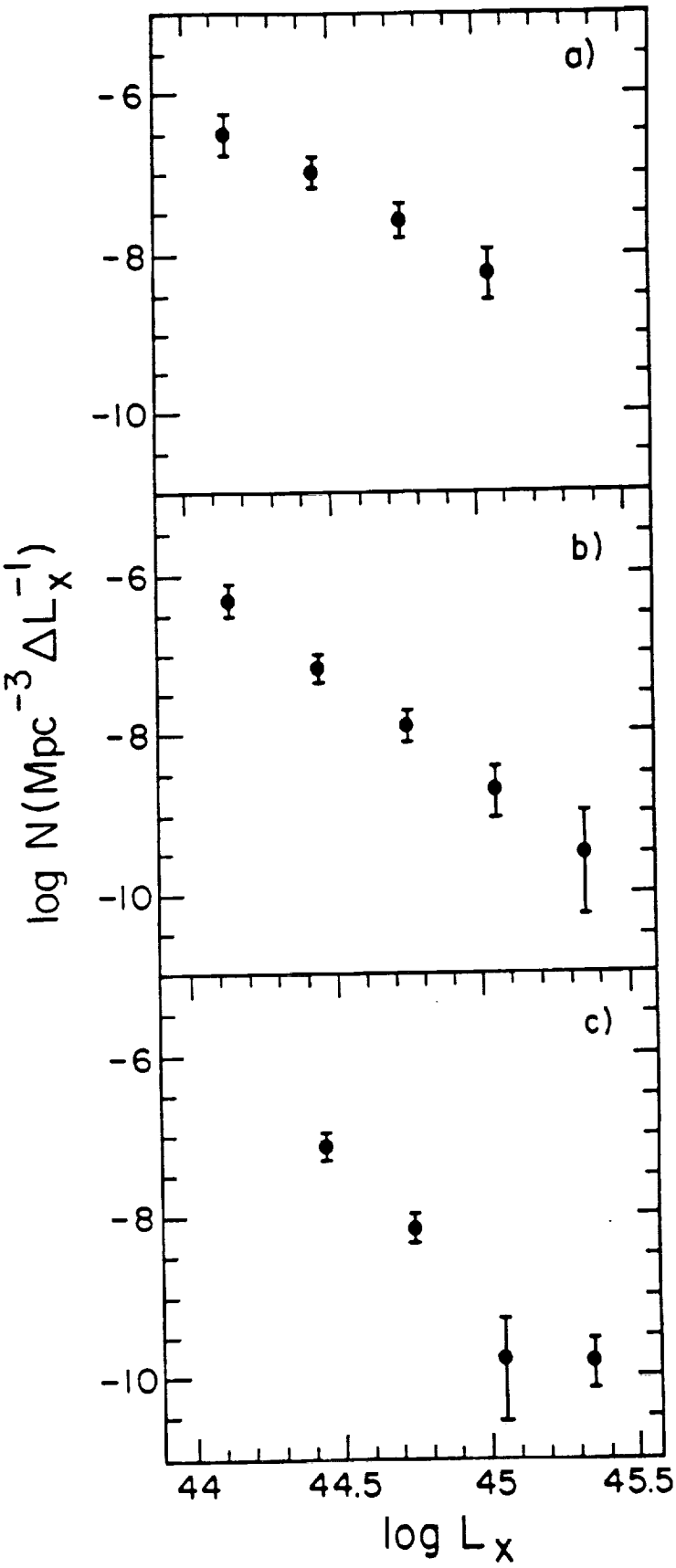

FIG. 1

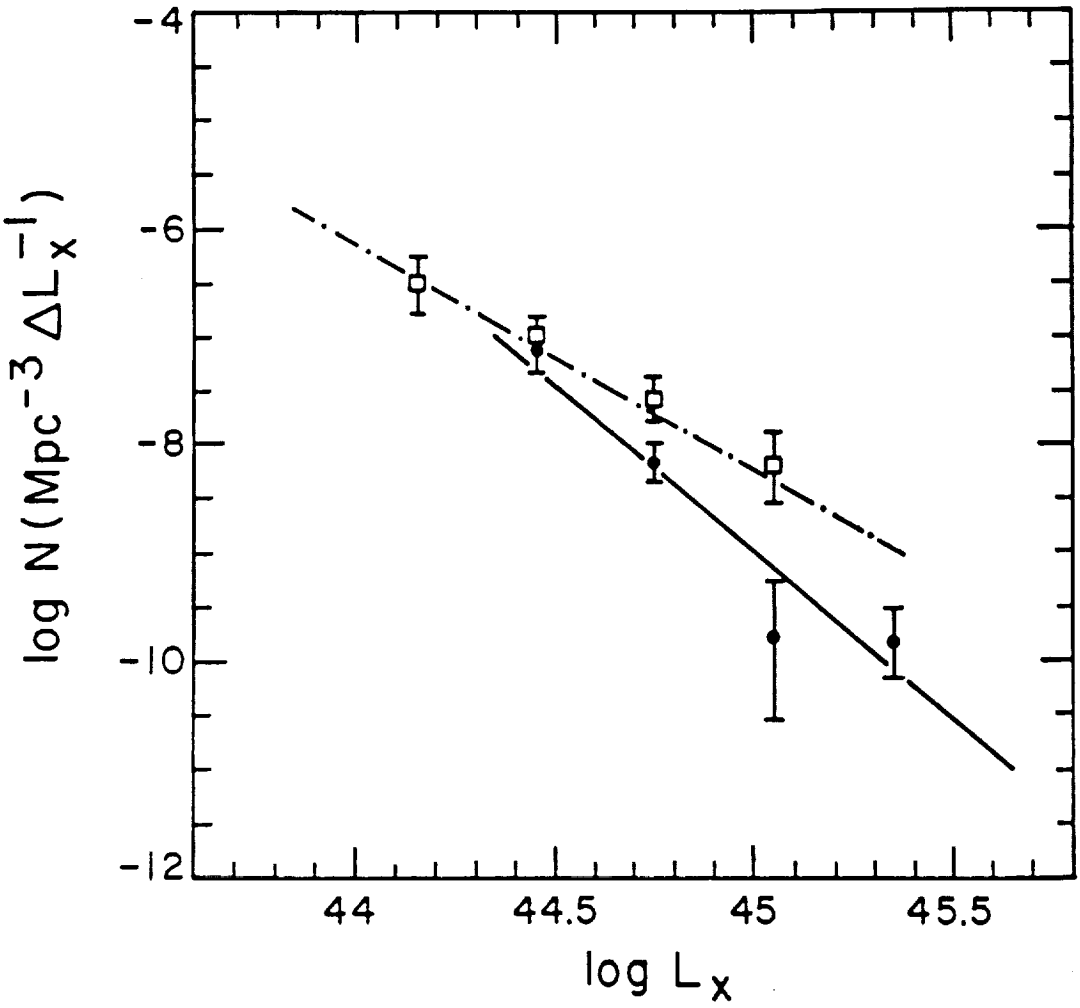

FIG. 2